

# Dynamics of pedogenic carbonate growth in the monsoonal tropical domain

Alexis Licht<sup>1</sup>, Julia R Kelson<sup>2</sup>, Shelly J. Bergel<sup>3</sup>, Andrew Schauer<sup>4</sup>, Sierra V Petersen<sup>5</sup>, Ashika Capirala<sup>4</sup>, Katharine W Huntington<sup>6</sup>, Guillaume Dupont-Nivet<sup>7</sup>, Zaw Win<sup>8</sup>, and Day Wa Aung<sup>9</sup>

<sup>1</sup>CEREGE, University of Aix-Marseille, France

<sup>2</sup>Department of Earth and Environmental Sciences, University of Michigan,

<sup>3</sup>University of Texas at Austin

<sup>4</sup>University of Washington

<sup>5</sup>University of Michigan-Ann Arbor

<sup>6</sup>University of Washington, Seattle, WA

<sup>7</sup>French National Centre for Scientific Research (CNRS)

<sup>8</sup>Department of Geology, University of Shwebo

<sup>9</sup>Department of Geology, University of Yangon

November 22, 2022

## Abstract

Pedogenic carbonate is widespread at mid latitudes where combined warm and dry conditions favor soil carbonate growth from spring to fall. The mechanisms and tempo of pedogenic carbonate formation are more ambiguous in the tropics, where longer periods of soil water saturation and higher soil respiration enhance calcite dissolution. This paper provides bulk and clumped isotope values from Quaternary and Miocene pedogenic carbonates in the tropical monsoonal domain of Myanmar where annual rainfall reaches up to 1700 mm. We show that carbonate growth in Myanmar is delayed to the coldest months of the year by sustained rainfall from mid spring to late fall. We propose that high soil moisture year-round in the tropical domain makes carbonate growth more episodic than in temperate ecosystems, and particularly sensitive to the seasonal distribution of rainfall. This sensitivity is also enhanced by high winter temperatures, allowing carbonate growth to occur outside the warmest months of the year. This high sensitivity is expected to be more prominent in the geological record during times with higher temperatures and greater expansion of the tropical realm. The winter bias in TD47 values found in Burmese soils, unique for pedogenic carbonates, constitute a potential signature for past tropical monsoonal (warm summer-wet) climates in paleosols, and are also found in our Miocene samples.



**22 Abstract:**

23 Pedogenic carbonate is widespread at mid latitudes where combined warm and dry conditions favor soil  
24 carbonate growth from spring to fall. The mechanisms and tempo of pedogenic carbonate formation are more  
25 ambiguous in the tropics, where longer periods of soil water saturation and higher soil respiration enhance  
26 calcite dissolution. This paper provides bulk and clumped isotope values from Quaternary and Miocene  
27 pedogenic carbonates in the tropical monsoonal domain of Myanmar where annual rainfall reaches up to  
28 1700 mm. We show that carbonate growth in Myanmar is delayed to the coldest months of the year by  
29 sustained rainfall from mid spring to late fall. We propose that high soil moisture year-round in the tropical  
30 domain makes carbonate growth more episodic than in temperate ecosystems, and particularly sensitive to  
31 the seasonal distribution of rainfall. This sensitivity is also enhanced by high winter temperatures, allowing  
32 carbonate growth to occur outside the warmest months of the year. This high sensitivity is expected to be  
33 more prominent in the geological record during times with higher temperatures and greater expansion of the  
34 tropical realm. The winter bias in  $\text{T}\Delta_{47}$  values found in Burmese soils, unique for pedogenic carbonates,  
35 constitute a potential signature for past tropical monsoonal (warm summer-wet) climates in paleosols, and  
36 are also found in our Miocene samples.

**37 Plain Language Summary**

38 Soil carbonates are the focus of numerous paleoenvironmental studies because their isotopic composition  
39 records many features of the local environment (such as the type and density of vegetation, annual or warm  
40 season temperatures, and aridity). Soil carbonates are commonly studied in temperate and arid areas; in those  
41 environments, carbonates form during warm months when soils dry. Soil carbonates are rarer but present in  
42 the tropics, where they have been barely studied. This study provides stable isotopic data from soil  
43 carbonates in the tropical monsoonal domain of Myanmar. We show that these soil carbonates grow during  
44 the coldest months of the year and follow different dynamics and isotope systematics than those of temperate  
45 and arid areas. We show that high soil wetness and warm temperatures year-round make carbonate growth  
46 particularly sensitive to the seasonal distribution of rainfall in the tropical domain. This seasonal sensitivity  
47 complicates the interpretation of soil isotopic data from past tropical ecosystems. We suggest that isotopic  
48 data from tropical paleoenvironments can be used as a proxy to reconstruct past rainfall distribution instead  
49 of average (or summer) environmental features.

50

**51 1. Introduction**

52 Soil carbonates are widespread from low to high latitudes, today and in the sedimentary archives, making  
53 them a valuable record of paleoenvironmental change through geologic time (e.g. Quade et al., 2011; Caves  
54 et al., 2015; Page et al., 2019; Xiong et al., 2020). However, most studies that investigate the features and  
55 growth dynamics of modern pedogenic carbonates have focused on temperate and (semi-)arid soils at mid  
56 latitudes, where calcic soils are abundant (e.g. Kelson et al., 2020). The dynamics of carbonate growth in the  
57 tropics remain barely explored, and it is unclear when and how tropical carbonates grow.

58 Soil carbonate grows in soils where  $\text{Ca}^{2+}$  is available and usually accumulates through multiple events of  
59 precipitation and dissolution that are controlled by soil water content, temperature, and  $\text{CO}_2$  concentration  
60 (Breecker et al., 2009; Huth et al., 2019). Carbonate precipitation is favored during warm and dry times  
61 because high soil temperatures decrease calcite solubility while evaporation increases calcium activity in the  
62 soil water (Gallagher and Sheldon, 2016; Fischer-Femal and Bowen, 2021). By contrast, carbonate  
63 dissolution is favored during wetter periods, especially during the plant growing season with high soil  
64 respiration and soil  $\text{CO}_2$  maxima (Breecker et al., 2009). Soil carbonate growth temperatures reconstructed  
65 using clumped isotope thermometry ( $T_{\Delta 47}$ ) commonly show higher values than the Mean Annual  
66 Temperature (MAT) in temperate and (semi-)arid ecosystems, supporting a warm-season bias in carbonate  
67 growth (Kelson et al., 2020). This warm bias relative to mean annual air temperatures is sometimes enhanced  
68 in arid and semi-arid environments (with commonly  $< 500$  mm of annual rainfall): solar heating increases  
69 summer soil temperatures relative to air temperature where soil surface is bare, while winter snow cover can  
70 mute winter soil temperatures (Gallagher et al., 2019).

71 Pedogenic carbonates are rarer at low latitudes but can be found in tropical seasonal areas (areas with  
72 average monthly temperatures above  $18^\circ\text{C}$  and at least one month with less than 60 mm of rainfall, sensu the  
73 Köppen classification), including close to the equator (Bettis et al., 2009). The mechanisms favoring soil  
74 carbonate formation and preservation in these warmer and wetter ecosystems are currently unclear given that  
75 higher soil respiration and longer periods of soil water saturation in tropical areas promote carbonate  
76 dissolution. In particular, the warm-season bias for carbonate growth may be less likely in the tropical  
77 monsoonal domain as warm temperatures in the late spring and summer are associated with intense rainfall,  
78 soil water saturation, and high soil respiration. In some regions with high summer rainfall outside the tropical  
79 domain, the carbonate growth season is delayed towards the fall such as in the Andes (Peters et al., 2013),  
80 but other regions such as Tibet do not show the same pattern (Quade et al., 2013; Burgener et al., 2018). A  
81 summer season bias for pedogenic carbonate growth remains the assumption of most studies using bulk and  
82 clumped isotope proxies on paleosols, including in the Asian monsoonal domain (Quade et al., 2011; Hoke et  
83 al., 2014; Ingalls et al., 2018; Botsyun et al., 2019; Xiong et al., 2020). This assumption is yet to be validated  
84 by a systematic study of soil carbonate growth in the tropics.

85 We address this discrepancy by providing an expanded dataset of bulk and clumped isotope values from  
86 Quaternary and Miocene soil carbonates in the tropical monsoonal domain of Myanmar, at sites where  
87 annual rainfall currently spans from 600 to 1700 mm. Our clumped and stable isotopic data indicate that  
88 carbonate growth varies locally from early winter to early spring. We explore the mechanisms leading to  
89 these cold  $T_{\Delta 47}$  values, unique so far in pedogenic carbonates, and highlight that soil carbonates grown under  
90 tropical climate follow different clumped and stable isotope systematics from their temperate and arid  
91 counterparts.

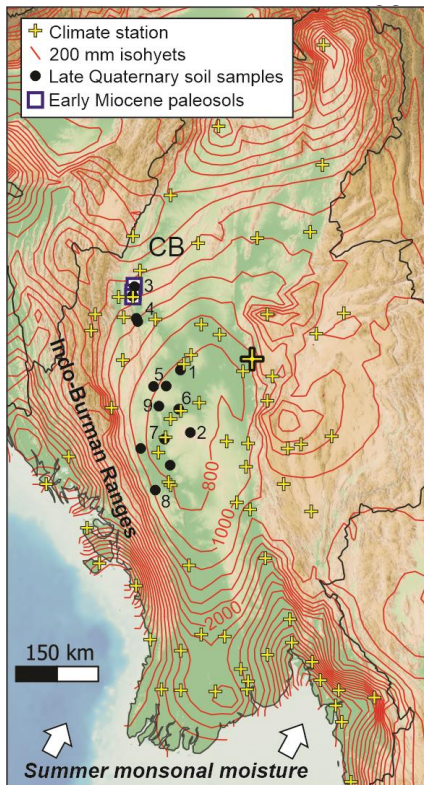


**Figure 1.** Map of western and central Myanmar with 200 mm isohyets of annual rainfall (red lines), Burmese climate stations (yellow crosses), Quaternary soil samples (black dots) and early Miocene paleosols (blue squares); numbers from 1 to 9 refer to sample location in Table 1. The location of the Mandalay climate station (Fig. 2a) is indicated with a bold cross. CB: Chindwin Basin.

## 2. Climate setting

Myanmar sits today in the South Asian monsoonal domain. Western Myanmar experiences intense summer rainfall (2-4 m from May to November) sourced from the Indian Ocean and amplified by the orographic effect of the Indo-Burman Ranges. Lying in the rainshadow of the ranges, the central Myanmar lowlands are located near sea-level and experience dramatic changes of Mean Annual Precipitation (MAP) over short distances, from 4 m in southern Myanmar to 600 mm in the “dry belt” of central Myanmar (Fig. 1). In contrast, the lowlands experience little regional temperature variation in monthly

107

108 temperatures ( $\pm 3^{\circ}\text{C}$  of variation among climate stations). Mean Annual Temperature (MAT) ranges from 23  
 109 to  $28^{\circ}\text{C}$ ; winter monthly temperatures average 17 to  $22^{\circ}\text{C}$ , with minima of  $10\text{--}15^{\circ}\text{C}$ ; average monthly  
 110 temperatures peak at  $30\text{--}33^{\circ}\text{C}$  in April-May, with average monthly maxima of  $40^{\circ}\text{C}$ . Temperatures remain  
 111 high (between  $27$  and  $30^{\circ}\text{C}$ ) during the rainy season, which spans all summer and fall (Fig. 2a). The area is  
 112 covered by mixed deciduous forests, woodlands, and savanna-woodlands. The vegetation is dominated by  
 113 C3 trees and shrubs with limited herbaceous ground cover; C4 plants represent ca. 25% of the herbaceous  
 114 vegetation (Khaing et al., 2019).

115 Unfortunately, there is no rainfall isotope data from the dry belt of central Myanmar. The closest station,  
 116 Yangon, experiences more intense rainfall ( $> 2$  m) and does not provide data outside the monsoon season  
 117 (Fig. 2b); New Delhi, India, receives a relatively low amount of annual precipitation (ca. 800 mm, mostly in  
 118 JJA) and is the closest GNIP station with a similar monsoonal climate to the Burmese dry belt. Both stations  
 119 display increased isotopic depletion through the monsoonal season, reaching their lowest  $\delta^{18}\text{O}$  values ( $-8$  to  $-$   
 120  $9$  ‰ VSMOW) in September (New Delhi) and October (Yangon). Non-monsoonal rainfall (December to  
 121 May) in New Delhi is much more  $^{18}\text{O}$ -enriched:  $-3$  to  $+1$  ‰ VSMOW, similar to what is seen regionally in  
 122 South Asia (Araguas-Araguas et al., 1998). Therefore, we estimate the isotopic composition of rainfall in our  
 123 study region to follow a similar seasonal pattern.

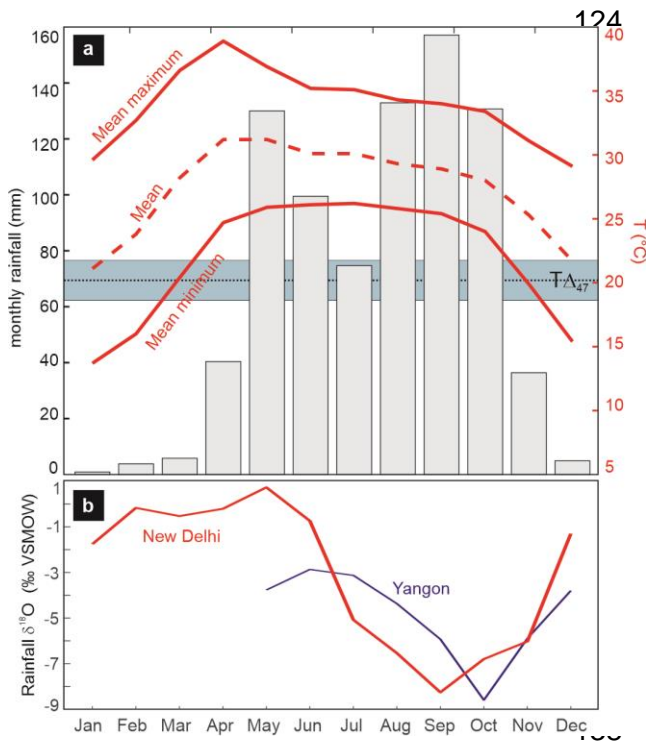


**Figure 2.** (a) Mean, mean maximum, and mean minimum monthly air temperatures (in red) and mean monthly precipitation (bars) in Mandalay (MAT: 27°C; MAP: 891 mm), displayed with the weighted average  $T\Delta_{47}$  and standard error (2 SE) of all Burmese samples (in green). Mean temperature data are from the global historical climatology network monthly temperature dataset, version 4 (Menne et al., 2018); temperature maxima, minima, and rainfall data from Lai Lai Aung et al. (2017); all climatic data are also available in Supplementary Table 1. (b) Monthly rainfall  $\delta^{18}O$  in Yangon and New Delhi; data from the Global Network of Isotopes in Precipitation (GNIP); only May to December data are available in Yangon.

139

### 140 3. Methods

141 Our field investigations in central Myanmar show that pedogenic carbonates are widespread in the central  
 142 dry belt and can be found in areas with up to 1.7 m of annual rainfall. We collected pedogenic carbonates  
 143 from 15 localities along road cuts and badlands, in poorly developed soils (inceptisols) to ensure their young  
 144 age. Three localities are soils developed on recent, loose river alluvium (including one on former farmland),  
 145 and one locality on Mount Popa volcanics attributed to the early Holocene (Belousov et al., 2018). The  
 146 other localities are soils developed on tilted Eocene, Miocene and Pliocene sedimentary rocks; considering  
 147 the recent deformation history of the central Myanmar lowlands (Plio-Pleistocene; Pivnik et al., 1998) and  
 148 the current high denudation rates in the central dry belt during the monsoon season (Stamp, 1940), these soils  
 149 are attributed to the Quaternary. Seasonal temperatures and rainfall amount at the 15 localities were obtained  
 150 from three sources: 1) outputs from the WorldClim 2.1 model at 5 minutes spatial resolution (Fick and  
 151 Hijmans, 2017); 2) variables from the closest climate station in central Myanmar (for monthly temperature  
 152 maxima, minima, and rainfall amount; Fig. 1); and 3) variables at the locality extrapolated from Burmese  
 153 climate stations with triangle-based cubic interpolation. The three approaches yield very similar results for  
 154 monthly and annual variables (Supplementary Table 1).

155 Carbonate nodules were sampled at depths greater than 50 cm; up to five nodules per locality were selected  
 156 for  $\delta^{18}O$  and  $\delta^{13}C$  analysis; samples were powdered and analyzed on a Kiel III Carbonate Device coupled to  
 157 a Finnigan Delta Plus isotope ratio mass spectrometer at the University of Washington. Clumped isotope  
 158 analysis was performed on one to two carbonate samples from ten of the localities, with 4-11 replicates each;  
 159 ten samples were analyzed at the University of Washington (digestion in a common acid held at 90 °C,  
 160 purification on an off-line vacuum system, and analysis on a MAT 253, following Kelson et al., 2017) and at

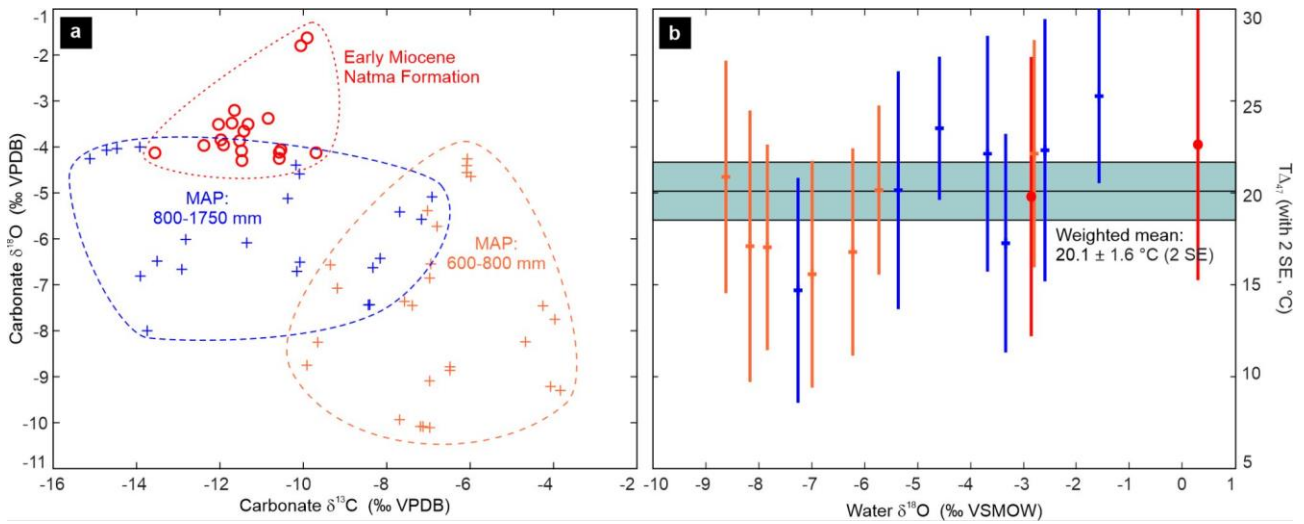
161 the University of Michigan (digestion and purification in a NuCarb automated sample preparation device  
162 held at 70 °C, and analysis on a Nu Perspective). The resulting  $\Delta_{47}$  values are standardized to the InterCarb  
163 framework (Bernasconi et al., 2021) and are converted to clumped isotope temperatures ( $T\Delta_{47}$ , in °C)  
164 following Anderson et al. (2021). Soil water  $\delta^{18}\text{O}$  is then calculated from carbonate  $T\Delta_{47}$  and  $\delta^{18}\text{O}$  values  
165 using the equation of Kim and O'Neil (1997).

166 We calculated soil  $\text{CO}_2$   $\delta^{13}\text{C}$  isotopic composition at each site from their average carbonate  $\delta^{13}\text{C}$  value, using  
167 the T-dependent fractionation equation of Romanek et al. (1992) and an estimate of soil temperature during  
168 carbonate growth. These estimates were obtained from either the  $T\Delta_{47}$  value at the site, the average  $T\Delta_{47}$   
169 value if two measurements were made at the site, or the average  $T\Delta_{47}$  value at all localities (20.1 °C; cf next  
170 section) if no clumped isotopic data were acquired. Finally, for eleven of the localities, we acquired solid  
171 organic matter  $\delta^{13}\text{C}$  values from decarbonated material from the carbonate layers. Solid samples were left  
172 overnight with 6M HCl in an oven at 60-80°C and rinsed with DI water the following day, and thus for three  
173 consecutive days;  $\delta^{13}\text{C}$  values of decarbonated material were acquired with a Costech Elemental Analyzer,  
174 Conflo III, MAT253 in continuous flow mode at the University of Washington.

175 We also sampled pedogenic nodules from the upper lower Miocene to lowermost middle Miocene Natma  
176 Formation in the Chindwin Basin, close to our wettest localities (modern MAP: ca. 1700 mm; Fig. 1). The  
177 Natma Formation consists of fluvial deposits rich in paleosols (mostly cumulative argillisols and rare  
178 argillic calcisols) and fossil wood specimens typical of moist deciduous to (semi-)evergreen forests found in  
179 monsoonal Southeast Asia (Gentis et al., 2019; Westerweel et al., 2020). Thirty samples from seven  
180 localities were prepared in thin section and examined using polarized light microscopy to evaluate the  
181 absence of secondary, sparitic calcite. Nineteen of these pedogenic carbonate samples were analyzed for  
182 carbon and oxygen isotopes; two samples were almost devoid of sparite and selected for clumped isotope  
183 analysis at the University of Washington (microphotographs of thin sections available in Supplementary File  
184 1). We also acquired solid organic material  $\delta^{13}\text{C}$  values from decarbonated material of the carbonate layers  
185 for four of the localities.

186 Location of samples, soil and paleosol details (sampling depth, soil texture and vegetation cover), and  
187 climate variables at the site and at the nearest climate stations are given in Supplementary Table 1; a  
188 synthesis of clumped isotope data is provided in Table 1; detailed bulk and clumped isotope results together  
189 with analytical procedures are given in Supplementary Table 2, and microphotographs of thin sections in  
190 Supplementary file 1. Raw clumped isotopic data from the University of Washington and University of  
191 Michigan are given in Supplementary Tables 3 and 4.

## 192 **4. Results**



193  
 194 **Figure 3. (a)** Oxygen and carbon isotopic composition of pedogenic carbonates from central Myanmar.  
 195 Quaternary samples (crosses) are sorted following the MAP at their locality: 600-800 mm (in orange), 800-  
 196 1750 mm (in blue); early Miocene samples (circles) are displayed in red. **(b)**  $T\Delta_{47}$  values and water  $\delta^{18}\text{O}$   
 197 values of pedogenic carbonates from central Myanmar (color coding same as in a); the weighted mean and  
 198 weighted standard error (2 SE) for quaternary samples is displayed in gray. Error bars for  $T\Delta_{47}$  values are 2  
 199 SE of replicate analyses. Propagated  $T\Delta_{47}$  error in water  $\delta^{18}\text{O}$  values (always  $<0.8$  ‰ at 1 SE) is not shown  
 200 for simplicity.

201

202 We split the dataset of Quaternary carbonates into two climatic groups of even size for a balanced  
 203 comparison: samples from localities below and above 800 mm MAP. Localities with MAP below 800 mm (7  
 204 localities, 26 stable isotopic and 7 clumped isotopic data points) cover a wide range of carbonate  $\delta^{18}\text{O}$   
 205 values: from -4 to -10 ‰ VPDB, with an average of -7.6 ‰ (Fig. 3a). Carbonate  $\delta^{13}\text{C}$  values range between -  
 206 3 and -10 ‰ VPDB (average: -6.7 ‰).  $T\Delta_{47}$  values range from  $15 \pm 6$  °C to  $22 \pm 6$  °C (2 SE), with a  
 207 weighted average and standard error of  $18.7 \pm 2.2$  °C (2 SE; Fig. 3b). Water  $\delta^{18}\text{O}$  values reconstructed from  
 208  $T\Delta_{47}$  and carbonate  $\delta^{18}\text{O}$  values range from -3 to -9 ‰ VSMOW (average -6.6 ‰). In contrast, localities  
 209 with MAP above 800 mm (8 localities, 22 stable isotopic and 7 clumped isotopic data points) display more  
 210 enriched  $\delta^{18}\text{O}$  values, spanning from -4 to -8 ‰ VPDB, with an average at -5.8 ‰. Carbonate  $\delta^{13}\text{C}$  values are  
 211 much more depleted, from -7 to -14 ‰ VPDB (average: -11.0 ‰).  $T\Delta_{47}$  values range from  $15 \pm 6$  °C to  $25 \pm$   
 212  $5$  °C (2 SE), with a weighted average and standard error of  $21.4 \pm 2.1$  °C (2 SE). Water  $\delta^{18}\text{O}$  values  
 213 reconstructed from  $T\Delta_{47}$  values range from -2 to -7 ‰ VSMOW (average -4.0 ‰). The weighted average  
 214  $T\Delta_{47}$  value of both groups remains close to the weighted average of the complete population ( $20.1 \pm 1.6$  °C, 2  
 215 SE). Interestingly, samples with low water  $\delta^{18}\text{O}$  values are almost systematically associated with lower-than-  
 216 average  $T\Delta_{47}$  values, while samples with high water  $\delta^{18}\text{O}$  values are associated with the warmest  
 217 temperatures. Carbonates with  $\delta^{18}\text{O}$  values below -6 ‰ VSMOW (6 samples) have an average  $T\Delta_{47}$  value of  
 218  $16.9 \pm 2.5$  °C (2 SE), while less depleted samples (8 samples) have an average  $T\Delta_{47}$  value of  $22.0 \pm 1.9$  °C (2  
 219 SE). Finally, soil organic matter sampled in the carbonate layers at eleven localities displays  $\delta^{13}\text{C}$  values  
 220 ranging from -27 to -22 ‰ VPDB (Fig. 4), with no clear difference between groups. These values are typical

221 of the  $\delta^{13}\text{C}$  range for C3 flora outside tropical rainforests (Kohn, 2010), but do not reject a potential presence  
 222 of a small proportion of C4 plants (<20 %).

223 Samples from the Miocene Natma Formation (7 localities, 19 stable isotopic and 2 clumped isotopic data  
 224 points) display carbonate  $\delta^{18}\text{O}$  values between -3 to -5 ‰ VPDB (average: -3.6 ‰), with the exception of  
 225 one locality that displays more enriched values (between -1 and -2 ‰). Carbonate  $\delta^{13}\text{C}$  values range from -9  
 226 to -14 ‰ VPDB (average: -11.3 ‰).  $T\Delta_{47}$  values equal  $20 \pm 8$  °C and  $23 \pm 6$  °C (2 SE), with reconstructed  
 227 water  $\delta^{18}\text{O}$  values from -3 to 0 ‰ VSMOW. Lastly, soil organic matter at four localities displays  $\delta^{13}\text{C}$

228 values ranging from -26 to -24 ‰ VPDB, again typical of  
 C3 flora outside tropical rainforests (Fig. 4).

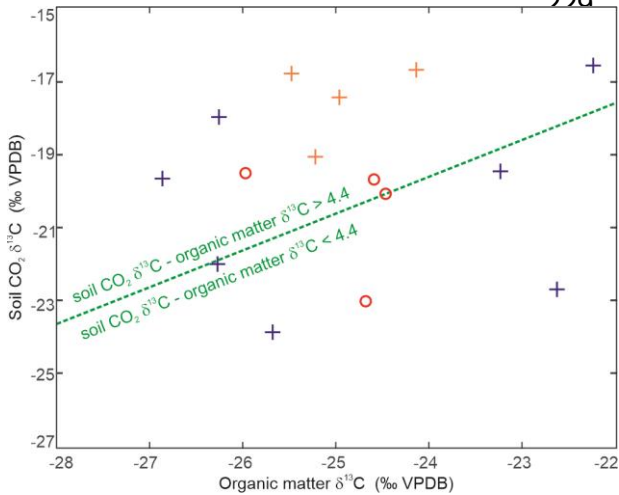


**Figure 4.** Organic matter  $\delta^{13}\text{C}$  values for the Quaternary and Miocene localities, compared to their calculated soil  $\text{CO}_2$   $\delta^{13}\text{C}$  values (see main text). Color coding is the same as Figure 3: Quaternary samples at localities with MAP < 800 mm (orange crosses), > 800 mm (blue crosses), and Miocene samples (red circles). The dashed green line highlights the domain where soil  $\text{CO}_2$   $\delta^{13}\text{C}$  = organic matter  $\delta^{13}\text{C}$  + 4.4 ‰, the minimum fractionation observed if soil carbonates and organic matter are contemporaneous (Cerling et al., 1991; Montanez, 2013).

239

Localities		Climate parameters from WorldClim V2, res 5min				Clumped isotopic data										
age	location on fig. 1	name	MAT (in °C)	WMMT (in °C)	CMMT (in °C)	MAP (in mm)	n	Carbonate $\delta^{13}\text{C}$ (‰ VPDB)	$\delta^{13}\text{C}$ S.E. (‰ VPDB)	Carbonate $\delta^{18}\text{O}$ (‰ VPDB)	$\delta^{18}\text{O}$ S.E. (‰ VPDB)	$\Delta_{47}$ Intercarb acid (‰)	$\Delta_{47}$ S.E. (‰)	$T\Delta_{47}$ (°C)	$T\Delta_{47}$ S.E. (°C)	Soil Water $\delta^{18}\text{O}$ (‰ VSMOW)
Quaternary soils	1	17NOD01	27.2	31.3	21.2	747	8	-6.08	0.02	-4.56	0.16	0.6904	0.0092	22.1	3.0	-2.8
	2	17NOD04	25.1	29.6	19.9	772	11	-6.97	0.04	-10.11	0.02	0.6943	0.0099	20.9	3.2	-8.6
	3	19NOD02	24.3	28.5	18.1	1701	6	-10.18	0.02	-4.39	0.03	0.6898	0.0107	22.3	3.5	-2.6
	3	19NOD03	24.3	28.5	18.1	1701	7	-10.16	0.03	-6.71	0.07	0.6965	0.0099	20.2	3.1	-5.3
	4	19NOD04	25.7	29.8	19.5	1372	9	-14.72	0.01	-4.07	0.03	0.7056	0.0097	17.3	3.0	-3.3
							4	-13.92	0.01	-4.00	0.02	0.6806	0.0073	25.4	2.4	-1.5
	5	19NOD06	25.7	30.0	20.0	845	7	-8.44	0.02	-7.44	0.03	0.7140	0.0099	14.7	3.0	-7.2
							6	-8.33	0.01	-6.63	0.07	0.6862	0.0059	23.5	2.0	-4.6
	6	19NOD07	27.6	31.9	22.1	647	10	-6.97	0.01	-6.85	0.03	0.7072	0.0092	16.8	2.8	-6.2
	5	19NOD08	27	31.3	21.3	720	10	-6.48	0.02	-8.86	0.13	0.7061	0.0121	17.1	3.7	-8.1
	7	19NOD09	27.3	31.6	21.9	655	7	-7.57	0.06	-7.36	0.07	0.7111	0.0099	15.6	3.0	-7.0
8	20NOD01	27	31.5	20.9	869	7	-7.70	0.09	-5.43	0.07	0.0096	0.0099	22.2	3.2	-3.6	
9	20NOD03	26.8	31.0	21.4	723	8	-9.89	0.02	-8.59	0.06	0.7063	0.0093	17.1	2.9	-7.9	
						4	-9.19	0.01	-7.07	0.03	0.6965	0.0073	20.2	2.3	-5.7	
Early Miocene	3	19NAT13	N/A				8	-9.70	0.48	-4.13	0.90	0.6976	0.0121	19.8	3.8	-2.8
	3	19NAT01	N/A				5	-9.91	0.06	-1.63	0.05	0.6881	0.0091	22.9	3.0	0.3

240  
 241 **Table 1.** Synthesis of clumped isotope data and soil water  $\delta^{18}\text{O}$  at each locality; climatic parameters from

242 Worldclim V2 at 5 minutes resolution; alternate climate parameters and soil morphology at every locality  
243 described in Supplementary Table 1, detailed clumped isotope data in supplementary Table 2.  $n$  = number of  
244 replicates;  $T\Delta_{47}$  values are calculated with a temperature- $\Delta_{47}$  relationship of Anderson et al. (2021). Soil  
245 water  $\delta^{18}\text{O}$  values are calculated from carbonate  $\delta^{18}\text{O}$  and  $T\Delta_{47}$  values using the equation of Kim and O'Neil  
246 (1997). Propagated  $T\Delta_{47}$  error in water  $\delta^{18}\text{O}$  values range from 0.8 to 1.6 ‰ (2 SE).

## 247 **5. Discussion**

### 248 **5.1 A record of multiple glacial and interglacial periods?**

249 The average  $T\Delta_{47}$  value ( $20.1 \pm 1.6$  °C, 2 SE) is only reached today in central Myanmar during winter (DJF;  
250 Fig. 1). The  $T\Delta_{47}$  values of some individual sites are colder on average than winter temperatures ( $15 \pm 6$  °C,  
251 2 SE), but still overlap with the Coldest Month Mean Temperature (CMMT) at the study sites (17-22 °C).  
252 This misfit suggests that these soil carbonates formed, or partially formed, during colder periods of the  
253 Quaternary.

254 Carbon isotopic data also support the idea that some of the soil carbonates at the wetter sites might have  
255 formed at least partially during an earlier period or might integrate over a longer period of time (> several  
256 millennia) with varying environmental conditions. Soil  $\text{CO}_2$  has a carbon isotopic composition at least 4.4-  
257 4.2 ‰ higher than soil organic matter due to differences in diffusion between different  $\text{CO}_2$  isotopologues  
258 during soil respiration (Cerling et al., 1991). Differences lower than 4.4-4.2 ‰ are commonly explained as  
259 related to recent changes in soil organic matter because labile organic matter has a faster turnover rate than  
260 pedogenic carbonate growth (Montanez, 2013). Of the wet sites (MAP > 800 mm) for which we have  $\delta^{13}\text{C}$   
261 values of organic matter, more than half (4 out of 7) display soil  $\text{CO}_2$   $\delta^{13}\text{C}$  values that are less than 4.4 ‰  
262 higher than those of the soil organic matter (Fig. 4). These results indicate that carbonates at the wettest sites  
263 grew partly (or completely) from soil-respired  $\text{CO}_2$  and organic matter that was more  $^{13}\text{C}$ -depleted than  
264 currently, which supports an earlier origin for some of our samples. Plant carbon isotopic composition in  
265 monsoonal (sub)tropical forests mainly relates to habitat openness, with lowest  $\delta^{13}\text{C}$  values in areas with the  
266 lowest light availability (Ehleringer et al., 1987). At a broader spatial scale, plant carbon isotopic  
267 composition in C3 plant communities is linked to humidity, with lowest  $\delta^{13}\text{C}$  values in the wettest areas  
268 (Kohn, 2010). Therefore, more depleted soil-respired  $\text{CO}_2$  at the time of carbonate formation at the wettest  
269 sites indicates that these carbonates grew at least partially under denser forest cover than is present today,  
270 and possibly wetter conditions.

271 Surface temperatures were ca. 2-5°C lower in South Asia during the last glacial maximum (Saraswat et al.,  
272 2013; Liu et al., 2020); partial carbonate growth during previous glacial periods could thus explain the  
273 colder-than-winter values found in some of our samples. However, it is difficult to assess if the more forested  
274 and possibly wetter conditions do indeed correspond to the last glacial periods, as the past hydrological  
275 history of Myanmar is poorly understood. Climate simulations suggest an increase of annual rainfall over the  
276 Indo-Burman Ranges and western Myanmar during the last glacial period (Di Nezio et al., 2018),  
277 corroborated by higher erosion rates in the ranges (Colin et al., 2001). In contrast, speleothems in eastern

278 Myanmar (Shan-Thai Highlands) and Thailand suggest a ~60% decrease of monsoonal rainfall at that time  
279 (Liu et al., 2020). Human-mediated deforestation during the late Holocene also could have partly driven the  
280 observed discrepancy between carbonate and organic matter  $\delta^{13}\text{C}$  values. The two pre-Quaternary samples  
281 analyzed here yield  $T\Delta_{47}$  values (20 and 23 °C) similar to the weighted  $T\Delta_{47}$  average of our Quaternary  
282 samples. The two soil localities unequivocally attributed to the Holocene (19NOD07, developed on former  
283 farmland, and 17NOD04, developed on early Holocene volcanoclastics) yield similar temperatures (17 and  
284 21°C). This suggests that the integration of glacial temperatures in our Quaternary  $T\Delta_{47}$  values is not the  
285 main driver lowering our carbonate growth temperature record to coolest average monthly temperatures.  
286 Even by decreasing monthly temperatures of modern air by 2 to 5 °C, as expected during the last glacial  
287 period in South Asia, the average  $T\Delta_{47}$  temperature ( $20.1 \pm 1.6$  °C, 2 SE) remains within the range of  
288 monthly average temperatures during winter to early spring (December to April; e.g. Fig. 2a). Our  $T\Delta_{47}$   
289 values thus indicate a cold-season bias in carbonate growth, even when considering a potential integration of  
290 soil temperatures through multiple glacial and interglacial cycles.

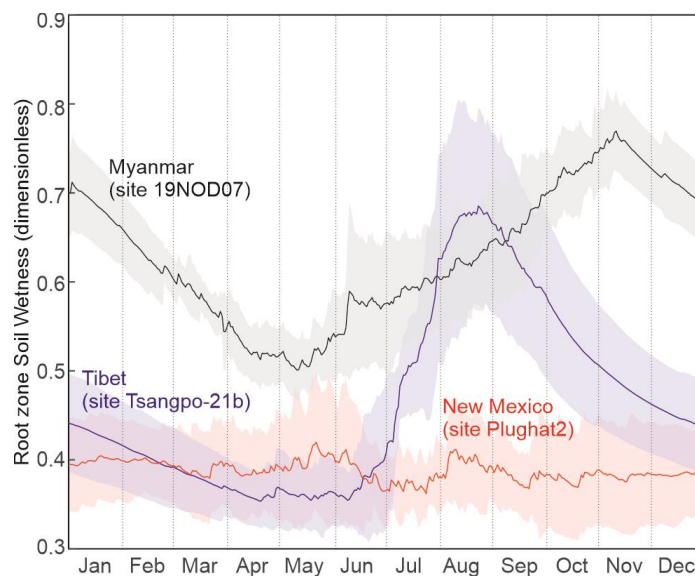
## 291 **5.2 Presence, mechanisms and timing of carbonate growth in the tropical domain**

292 The presence of soil carbonate in some of the wettest parts of central Myanmar, and their growth during  
293 possibly wetter conditions, is contrary to the traditional wisdom that soil carbonates do not form in  
294 environments with MAP > 1000 mm/year (Retallack, 2005). While this occurrence is rare, soil carbonates  
295 have been observed in “wet” localities such as northern India (Singh and Singh, 1972) and Tennessee, USA  
296 (Railsback, 2021). Quaternary pedogenic nodules are also found in multiple localities near the equator in  
297 Java (latitude ca. 7°N), in areas with prominent seasonality and modern annual rainfall exceeding 1700 mm  
298 (van Der Kaars and Dam, 1997; Bettis et al., 2009). Following Breecker et al. (2009, 2010), we propose that  
299 the intensely seasonal nature of precipitation and soil water content in Myanmar allows for preferential  
300 formation of carbonates during the dry season, in winter and early spring.

301 The long monsoonal season in Myanmar, with intense and steady rainfall from May until October (Fig. 2a),  
302 results in a delayed peak of soil moisture in late Fall (mid November; Fig. 5). In winter and spring  
303 (December to May), central Myanmar experiences little rainfall and monthly temperatures remain above  
304 15°C; these warm and dry conditions allow the soils to steadily dry until the onset of the next monsoon  
305 season. Pedogenic carbonates in this region are thus expected to form throughout the winter and spring,  
306 including through the spring months of April and May when monthly temperatures peak above 30°C, as soil  
307 drying continues to concentrate  $\text{Ca}^{2+}$  ions in the soil and promote saturation of calcite (Breecker et al., 2009).  
308 Our  $T\Delta_{47}$  values do indeed indicate that carbonate growth occurs here in the winter and spring, but in  
309 contrast display an apparent bias towards the earlier part of the dry season. This bias could partly result from  
310 an imprint of glacial temperatures, or alternatively suggests a narrow period of carbonate growth at the start  
311 of the seasonal dewatering phase. Specifically, this apparent bias in temperatures could be a result of two  
312 processes: 1) soil respiration may increase enough in late spring to reduce calcite precipitation and/or 2)  
313 carbonate that forms in later spring may be more sensitive to dissolution than winter-grown carbonates, as  
314 described in the following paragraphs.

315 (1) Soil respiration is primarily controlled by soil moisture in Asian monsoonal ecosystems, with low values  
 316 in the dry season and high values during the monsoon season (Kume et al., 2013, Hanpattanakit et al., 2015).  
 317 Winter months in central Myanmar display the lowest monthly rainfall amount (commonly <10 mm per  
 318 month from December to March; Fig. 2a). Sparse but heavy rain events during mid-spring (April-May) do  
 319 not impact the average soil moisture budget (Fig. 5) but could result in rain-induced soil respiration pulses,  
 320 as seen in other seasonal tropical forests (Rubio and Detto, 2017). These pulses of soil moisture and soil  
 321 respiration could prevent spring carbonate growth. In addition to this important moisture control, temperature  
 322 variations within the dry season sometimes secondarily impact soil respiration (Meena et al., 2020) and thus  
 323 the timing of carbonate growth. In this setting, mild temperatures in December and January could drive down  
 324 soil respiration, reducing soil CO<sub>2</sub> concentrations and favoring carbonate growth.

325 (2) Pedogenic carbonate that forms in late spring might not preserve as easily as earlier forming carbonate.  
 326 Late spring rain events or summer monsoonal rainfall could preferentially dissolve freshly-grown carbonates  
 327 and/or the outermost layers of older carbonates, leaving behind only the remnants of early, winter-grown  
 328 carbonates. The mechanisms for this potential bias in dissolution remain unclear, but could relate to varying  
 329 texture and/or soil depth between carbonates grown at different times of year.



330

331 **Figure 5.** Root zone (0-100 cm) soil wetness from SMAP L4 satellite data (Reichle et al., 2018) at three sites  
 332 with pedogenic carbonate clumped isotope data: Tsangpo-21b in Tibet (in blue; Burgener et al., 2018),  
 333 Plughat-2 in New Mexico (in red; Gallagher and Sheldon, 2016), and 19NOD04 in Myanmar (in black; this  
 334 study). Soil wetness unit (dimensionless) varies between 0 and 1, indicating relative saturation between  
 335 completely dry conditions and completely saturated conditions, respectively; satellite data span over the  
 336 2015-2020 period and were averaged daily (curve: average; shaded area: standard deviation).

337

338 A winter bias in carbonate growth contrasts the summer bias found in Tibetan carbonates, also grown under  
 339 a well-established monsoonal regime (Quade et al., 2013; Burgener et al., 2018). The soil annual  
 340 hydrological budget and temperature variation in Myanmar are significantly different from those of Tibet,

341 providing potential explanations for this discrepancy. Monsoonal rainfall in Tibet is less intense (MAP  
 342 commonly < 500 mm) and the rainy season is shorter. Soil wetness peaks in late summer (late August) and  
 343 soils quickly dry (Fig. 5), potentially allowing carbonate to grow in early Fall. Unlike in Myanmar, where  
 344 winter temperatures remain mild (CMMT > 15°C), Tibetan winter temperatures drop below freezing,  
 345 drastically inhibiting evaporation and evapotranspiration and decreasing calcium activity. Soil water freezing  
 346 favors cryogenic carbonate formation, which is associated with disequilibrium effects in clumped isotopic  
 347 composition and commonly drives  $T\Delta_{47}$  values up; the contribution of this process in Tibetan carbonates  
 348 remains debated (Burgener et al., 2018). A renewal of pedogenic carbonate growth in late spring and early  
 349 summer, as proposed by Quade et al. (2013), is additionally possible when soils defrost before the rainy

350 season.

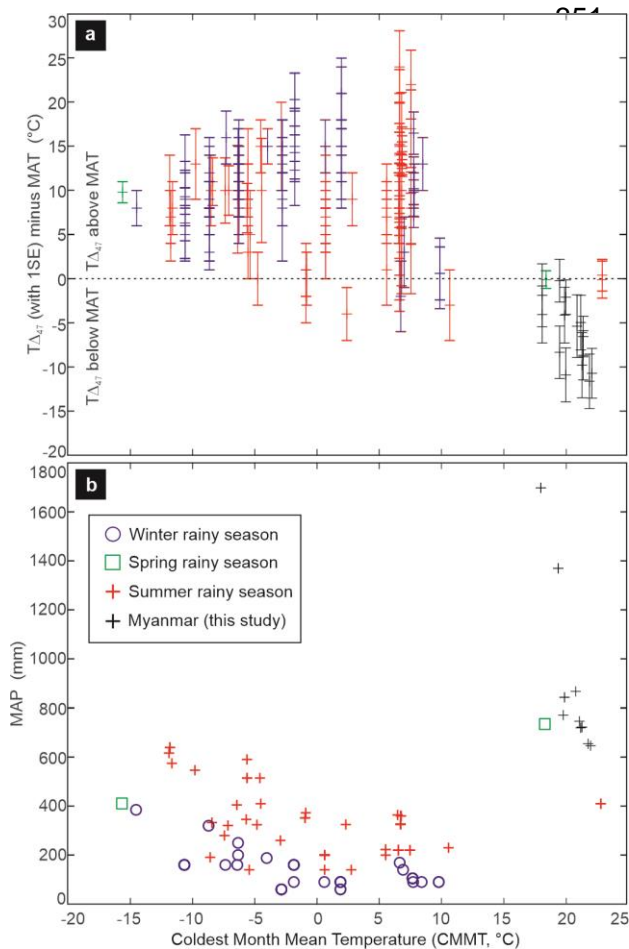


**Figure 6.** (a)  $T\Delta_{47}$  values minus MAT of the same sites compared to their Coldest Month Mean Temperature (CMMT);  $T\Delta_{47}$  error bars correspond to 1 SE.  $T\Delta_{47}$  values from previous sites are from Kelson et al. (2020); CMMT, MAT, and MAP of Burmese sites from Worldclim 2.1; CMMT, MAT, and MAP from other sites from Kelson et al. (2020) or Worldclim 2.1 if not provided. (b) CMMT and MAP at the study sites (black crosses) compared to previously published soil carbonate clumped isotope data (from Kelson et al., 2020). Previously published sites are sorted according to their prominent rainy season on both panels: winter (blue crosses), spring (green crosses) and summer (red crosses); color coding is the same for both panels.

370 The apparent winter bias recorded in the Burmese  
 371 pedogenic carbonates is so far unique in the clumped  
 372 isotopic record of Quaternary carbonates (Fig. 6a). This is likely because the Burmese samples presented  
 373 here represent an environment that is not previously addressed in clumped isotope studies, as this  
 374 environment is both wetter and warmer (as demonstrated by a high CMMT; Fig 6b). Most clumped isotope  
 375 data screened for robustness by Kelson et al. (2020) --more than 2 replicates, sampling depth >39 cm-- come  
 376 from localities with MAP < 500 mm and more evenly distributed rainfall than the monsoonal domain,  
 377 resulting in low levels of soil wetness year-round, even during the (weak) rainy season(s) (such as seen in the  
 American Southwest; Fig. 5). All previous clumped isotope data sites also display cold CMMT (< 10 °C),  
 which likely inhibits pedogenic carbonate growth during the cold season. Of the previously studied soil

378 carbonate localities, only those in Ethiopia and Kenya experience high CMMT (18-23 °C) similar to our  
379 Burmese sites (Passey et al., 2010). The Kenyan site experiences evenly distributed, moderate rainfall over  
380 the year, peaking in spring (MAP: 736 mm), while the Ethiopian localities are much drier (MAP: 410 mm)  
381 and go through two dry seasons, in winter and late spring-early summer. Both rainfall distributions likely  
382 favor multiple yearly episodes of carbonate growth. The  $T\Delta_{47}$  values at both sites are in agreement with  
383 MAT (Fig. 6b), but these sites have a narrow seasonal range of temperature variation ( $< \pm 4$  °C), and it is  
384 difficult to detect seasonal bias from  $T\Delta_{47}$  alone.

### 385 **5.3 Local parameters influencing carbonate growth and isotopic signature within the tropical domain**

386 The spread of oxygen and carbon isotopic data among our sites suggests that multiple local factors influence  
387 carbonate growth and its isotopic signature within the Burmese lowlands.

388 Evaporation in soils commonly drives carbonate  $\delta^{18}\text{O}$  values up and is more likely to occur under arid  
389 conditions (Cerling and Quade, 1993; Beverly et al., 2020). Spatial changes in evaporation effects have  
390 likely little impact on the spread of  $\delta^{18}\text{O}$  values in our dataset, as the most depleted carbonate  $\delta^{18}\text{O}$  values are  
391 only present at the drier sites of study. Interestingly, the coldest  $T\Delta_{47}$  values in our Quaternary record are  
392 associated with the lowest water  $\delta^{18}\text{O}$  values (-9 to -6 ‰ VSMOW; Fig. 3b), similar to rainfall  $\delta^{18}\text{O}$  values  
393 reached at the end of the monsoon season (Fig. 1b), while the warmest temperatures are associated with  
394 higher  $\delta^{18}\text{O}$  values (-6 to -1 ‰ VSMOW), typical of spring rainfall. These variations cannot be explained by  
395 differences in the ages of the pedogenic carbonates; carbonates grown during glacials --thus displaying the  
396 coldest temperatures-- would have higher water  $\delta^{18}\text{O}$  values than carbonate grown during interglacials, as  
397 documented in Burmese speleothems (Liu et al., 2020). The entire range of modern seasonal rainfall  $\delta^{18}\text{O}$   
398 values is covered in the range of calculated soil water  $\delta^{18}\text{O}$  values, suggesting the variation is due to  
399 differences in the seasonal timing of carbonate growth. Carbonates often prominently incorporate the  $\delta^{18}\text{O}$   
400 values of water that is contemporaneous with or directly preceding the period of carbonate growth rather  
401 than carry over soil water  $\delta^{18}\text{O}$  values from out-of-season (Gallagher and Sheldon, 2016; Fischer-Femal and  
402 Bowen, 2021). Accordingly, the coldest  $T\Delta_{47}$  values and most depleted  $\delta^{18}\text{O}$  values are compatible with  
403 carbonate growth in early winter with minimum soil water storage (1-3 months), incorporating late  
404 monsoonal waters; in contrast, warmer  $T\Delta_{47}$  values and higher  $\delta^{18}\text{O}$  values are compatible with growth in  
405 early spring, enriched due to incorporation of spring rainwater or evaporation (Fig 3b).

406 Based solely on soil water  $\delta^{18}\text{O}$  values, our limited dataset suggests that carbonate at drier sites (MAP <800  
407 mm) grows preferentially in winter while growth at wetter sites (MAP >800 mm) is delayed towards early  
408 spring (Fig. 3b). The uncertainty around  $T\Delta_{47}$  values remains too large to confirm that the same MAP-  
409 dependency is seen in growth temperatures. Individual carbonate nodules yield water  $\delta^{18}\text{O}$  values compatible  
410 with winter and spring rain composition at the same locality, together with a wide range of  $T\Delta_{47}$  values ( $15 \pm$   
411  $6$  and  $23 \pm 4$  °C 2 SE at site 19NOD06; Table 1), suggesting that MAP is not the only relevant factor  
412 impacting carbonate growth temperatures. Local (meter-scale) differences in landscape position, soil texture,  
413 or plant water use could impact soil water storage and explain some of the observed isotopic variability  
414 (Kelson et al., 2020).

415 The range of carbonate  $\delta^{13}\text{C}$  values is particularly wide: there is an 11 ‰ difference between the most  
416 depleted samples in the wet domain and the least depleted samples in the dry domain. This difference cannot  
417 be explained by a varying amount of C4 plants, as organic matter  $\delta^{13}\text{C}$  values do not show any marked  
418 contribution from C4 plants even at the driest sites (e.g.  $\delta^{13}\text{C}$  always  $< -20$  ‰ VPDB). Decreased water stress  
419 on Burmese C3 plants during glacials could potentially account for 3-5 ‰ of depletion in the pedogenic  
420 carbonates of the wetter sites (Kohn, 2010), but fails to explain the much wider range of  $\delta^{13}\text{C}$  values.  
421 Seasonal variations in soil respiration rate and/or isotopic composition significantly impact soil  $\text{CO}_2$   $\delta^{13}\text{C}$   
422 values (Breecker et al., 2009) and could potentially explain part of this difference, as already proposed for  
423 other past monsoonal C3 records (Licht et al., 2020). Low rates and high  $\delta^{13}\text{C}$  values of winter soil  
424 respiration followed by higher rates and lower  $\delta^{13}\text{C}$  values of early spring respiration could partly explain the  
425 observed difference between sites on both ends of the  $\delta^{13}\text{C}$  spectrum.

426 More generally, carbonate  $\delta^{13}\text{C}$  and  $\delta^{18}\text{O}$  values are not positively correlated as would be expected of arid  
427 regions, where the effects of soil evaporation and respiration are the main drivers in changing those values  
428 (Fischer-Femal and Bowen, 2020; Broz et al. 2021). We hypothesize that overall higher soil wetness year-  
429 round in central Myanmar minimizes this covariation in comparison to temperate carbonate-rich soils, while  
430 making the bulk and clumped isotope composition particularly sensitive to the seasonal rainfall distribution.  
431 Other eco-hydrological factors are likely also at play but remain to be identified with a more thorough  
432 sampling and systematic study of soil features. The soil texture, Bk horizon depth and dominant vegetation at  
433 each locality are described in Supplementary Table 1 and do not covary with bulk and clumped isotope  
434 composition (not shown). Importantly, Bk depth appears independent of local MAP, unlike observed in the  
435 temperate domain (Retallack, 2005). Our results thus highlight that carbonates grown under tropical  
436 conditions follow different growth patterns and isotope systematics than their temperate counterparts.

#### 437 **5.4 Implications for paleoenvironmental studies**

438 Our dataset illustrates the high bulk and clumped isotope variability found in a limited geographical area in  
439 the tropics (ca. 10 ‰ for C and O isotopic data and 10 °C for  $\text{T}\Delta_{47}$  values), driven by subtle changes in  
440 carbonate growth season influenced by local hydrological processes. This variability alone could explain a  
441 significant part of the variations found in several past bulk and clumped isotopic records without requiring  
442 dramatic changes of climate or elevation (Page et al., 2019). The processes and seasonal biases impacting  
443 carbonate growth in Myanmar today are also expected to be common in paleosols during Greenhouse  
444 intervals, which are associated with higher CMMT at mid-latitude, a wide spread of tropical ecosystems  
445 (Wing and Greenwood 1993; Toumoulin et al., 2021), and a more active hydrological cycle resulting in  
446 locally increased rainfall seasonality, as is seen in Paleogene Myanmar (Licht et al., 2014b). In particular,  
447 our results open the way for a reinterpretation of past bulk and clumped isotopic data used for the  
448 paleoaltimetry of Tibetan carbonates, which have so far systematically been interpreted as growing in  
449 summer or equally throughout the year (e.g. Botsyun et al., 2019); low stable isotopic values ( $< -10$  ‰  
450 VPDB) and cold  $\text{T}\Delta_{47}$  values ( $< 25$  °C) are, in this framework, considered as reflecting high elevation. While  
451 some Paleogene sites display reconstructed water  $\delta^{18}\text{O}$  values that are too low ( $< -14$  ‰ VPDB) to be solely

452 created by a monsoonal isotopic signature and thus require high elevations to explain them (Ingalls et al.,  
453 2020; Fang et al., 2020), others display bulk and clumped isotopic values similar to what we find today in  
454 Myanmar, and can alternatively reflect a monsoonal signature in carbonate growth at low elevation (Xiong et  
455 al., 2020). Moreover, decreasing rainfall amount and winter temperatures during gradual Tibetan uplift in the  
456 monsoonal domain should gradually move the carbonate growth season from early spring to winter, late fall,  
457 and eventually early fall and/or late spring, once the winters are too cold to favor carbonate growth and the  
458 rainy season is limited to a few months in the summer. This complex evolution makes paleoaltimetry  
459 estimates based on soil carbonate data more challenging in the monsoonal domain and for past tropical  
460 climates.

### 461 **5.5 An isotopic signature for past monsoonal regimes?**

462 While making paleoelevation estimates based solely on pedogenic carbonate bulk and clumped isotope data  
463 appears challenging, these data can provide unique insight into rainfall dynamics when MAT or elevation are  
464 independently constrained. In particular, the climatic patterns proposed as the origin of the Burmese winter  
465 bias in  $T\Delta_{47}$  values, i.e. wet summers combined with dry and warm winters, are diagnostic of monsoonal  
466 areas at low altitude. Lower  $T\Delta_{47}$  values than MAT should thus provide a proxy for tropical monsoonal  
467 climate. In addition, our observations suggest that C and O isotopic data could potentially provide insights  
468 into rainfall amount, though their MAP-dependency remains to be confirmed with a more systematic study  
469 of Quaternary tropical pedogenic carbonates and soil waters.

470 In this light, the results from the Miocene Natma Formation are meaningful and provide a proof-of-concept  
471 example for the usefulness of combined bulk and clumped isotope analysis in the tropical domain when the  
472 climate is independently constrained. Natma pedogenic carbonates yield low  $T\Delta_{47}$  values (20-23 °C), high  
473  $\delta^{18}\text{O}$  (>-4 ‰ VPDB) and low  $\delta^{13}\text{C}$  (< -10 ‰ VPDB) values. Following regular isotopic interpretative keys  
474 used in the temperate domain,  $T\Delta_{47}$  values could be interpreted as reflecting colder summers than today's  
475 (Kelson et al., 2020), and high  $\delta^{18}\text{O}$  values would reflect less monsoonal rainfall while low  $\delta^{13}\text{C}$  would mean  
476 overall wetter conditions (Caves et al., 2015). These interpretations suggest a colder and wetter climate at the  
477 time of the Natma Formation, with limited monsoons and more evenly distributed rainfall over the year.  
478 They contrast with independent lines of evidence for a warmer late early to early middle Miocene globally  
479 (Steinthorsdottir et al., 2020) with intense Asian monsoons (Clift et al., 2008), and raise preservation issues,  
480 as higher but less seasonal rainfall would likely favor the dissolution of pedogenic carbonate. In contrast,  
481 fossil wood specimens of the Natma Formation reflect different ecotones of seasonal forests with coastal,  
482 mixed to dry deciduous, and wet evergreen species, suggesting a warm, seasonal monsoonal climate during  
483 the late early Miocene at least as wet as today, and possibly wetter summers (Gentis et al., 2019). In this  
484 context, low  $T\Delta_{47}$  values (<25 °C) in Natma pedogenic carbonates corroborate a summer rainy season (Fig.  
485 3b), while high  $\delta^{18}\text{O}$  (>-4 ‰ VPDB) values and low  $\delta^{13}\text{C}$  (< -10 ‰ VPDB) values fall on the "wet" side of  
486 the carbonate spectrum, similar to what is found today at the sampling site (Fig. 3a). This interpretation is  
487 more in line with the fossil wood assemblage, and suggests modern-like monsoonal rainfall in Myanmar in  
488 the late early Miocene. This example illustrates how different isotopic systematics are between pedogenic

489 carbonates in the temperate and tropical domains, and how applying inadequate interpretative keys can  
490 significantly impact paleoclimatic interpretations.

## 491 **6. Conclusion**

492 Low  $T\Delta_{47}$  values ( $<25$  °C) in Quaternary soil carbonates from central Myanmar indicate a bias in carbonate  
493 growth timing toward winter and early spring. We attribute the cold season bias to the combined effects of  
494 warm winter temperatures and intense rainfall during the summer and fall, conditions that are typical of  
495 tropical monsoonal climates. These conditions allow for carbonate growth in areas where MAP today  
496 exceeds 1700 mm. Oxygen and carbon isotopic data suggest that carbonate growth timing locally varies from  
497 early winter to early spring, with decreasing incorporation of depleted oxygen from monsoonal waters  
498 throughout the growth span. This trend is partly influenced by local MAP, with the wettest sites possibly  
499 delayed to early spring. Our results confirm that rainfall annual distribution and amount significantly impact  
500 the season of carbonate growth and its bulk and clumped isotopic record (Peters et al., 2013; Gallagher and  
501 Sheldon, 2016; Burgener et al., 2016; Kelson et al., 2020). We suggest that this expression is particularly  
502 important in tropical areas, where high soil wetness year-round makes carbonate growth more episodic and  
503 particularly sensitive to the seasonal distribution of rainfall. This sensitivity is also enhanced by high  
504 CMMT, allowing carbonate growth to move outside the warmest months of the year. This high sensitivity is  
505 expected to be more prominent in the geological record during times with higher temperatures and greater  
506 expansion of the tropical realm. “Cold”  $T\Delta_{47}$  records in Asian paleosols, often interpreted through the lense  
507 of evolving topography, might instead provide a possible fingerprint for tropical monsoonal climate. Our  
508 understanding of pedogenic carbonate growth dynamics has been so far strongly biased toward temperate  
509 ecosystems; our results show that pedogenic carbonates grown under Burmese tropical conditions follow  
510 different dynamics and isotope systematics. These remain to be further documented and expanded to other  
511 tropical soil carbonates to gain a more complete understanding of their growth under different conditions and  
512 the resulting implications for paleoenvironmental reconstructions.

513

## 514 **Acknowledgments**

515 This study was financially supported by the University of Washington and European Research Council  
516 consolidator grant MAGIC 649081. We thank L. Burgener, J. Harlé, S. Shekut, C. Bourgeois, Kyi Kyi  
517 Thein, Hnin Hnin Swe, Myat Kay Thi, A. Gough, D. Perez-Pinedo, J. Westerweel, and P. Roperch for  
518 prolific discussions and assistance in the field and lab. Datasets for this research are included in the  
519 supplementary information files and archived on EarthChem (to be released upon publication).

520

## 521 **References**

522 Anderson, N. T., Kelson, J. R., Kele, S., Daëron, M., Bonifacie, M., Horita, J., ... & Bergmann, K. D. (2021).  
523 A unified clumped isotope thermometer calibration (0.5–1100° C) using carbonate-based standardization.

- 524 *Geophysical Research Letters*, e2020GL092069.
- 525 Araguás-Araguás, L., Froehlich, K., & Rozanski, K. (1998). Stable isotope composition of precipitation over  
526 southeast Asia. *Journal of Geophysical Research: Atmospheres*, 103(D22), 28721-28742.
- 527 Belousov, A., Belousova, M., Zaw, K., Streck, M. J., Bindeman, I., Meffre, S., & Vasconcelos, P. (2018).  
528 Holocene eruptions of Mt. Popa, Myanmar: Volcanological evidence of the ongoing subduction of Indian  
529 Plate along Arakan Trench. *Journal of Volcanology and Geothermal Research*, 360, 126-138.
- 530 Broz, A., Retallack, G. J., Maxwell, T. M., & Silva, L. C. (2021). A record of vapour pressure deficit  
531 preserved in wood and soil across biomes. *Scientific reports*, 11(1), 1-12.
- 532 Bernasconi, S., Daëron, M., Bergmann, K., Bonifacie, M., Meckler, A. N., Affek, H., ... & Ziegler, M.  
533 (2021). InterCarb: A community effort to improve inter-laboratory standardization of the carbonate clumped  
534 isotope thermometer using carbonate standards.
- 535 Bettis III, E. A., Milius, A. K., Carpenter, S. J., Larick, R., Zaim, Y., Rizal, Y., ... & Bronto, S. (2009). Way  
536 out of Africa: Early Pleistocene paleoenvironments inhabited by *Homo erectus* in Sangiran, Java. *Journal of*  
537 *Human Evolution*, 56(1), 11-24.
- 538 Beverly, E., Levin, N. E., Passey, B. H., Aron, P. G., Yarian, D. A., Page, M., & Pelletier, E. M. (2020).  
539 Triple oxygen and clumped isotopes in modern soil carbonate along an aridity gradient in the Serengeti,  
540 Tanzania. *Earth and Space Science Open Archive ESSOAr*.
- 541 Botsyun, S., Sepulchre, P., Donnadiou, Y., Risi, C., Licht, A., & Rugenstein, J. K. C. (2019). Revised  
542 paleoaltimetry data show low Tibetan Plateau elevation during the Eocene. *Science*, 363(6430).
- 543 Breecker, D. O., Sharp, Z. D., & McFadden, L. D. (2009). Seasonal bias in the formation and stable isotopic  
544 composition of pedogenic carbonate in modern soils from central New Mexico, USA. *Geological Society of*  
545 *America Bulletin*, 121(3-4), 630-640.
- 546 Breecker, D. O., Sharp, Z. D., & McFadden, L. D. (2010). Atmospheric CO<sub>2</sub> concentrations during ancient  
547 greenhouse climates were similar to those predicted for AD 2100. *Proceedings of the National Academy of*  
548 *Sciences*, 107(2), 576-580.
- 549 Burgener, L., Huntington, K. W., Hoke, G. D., Schauer, A., Ringham, M. C., Latorre, C., & Díaz, F. P.  
550 (2016). Variations in soil carbonate formation and seasonal bias over > 4 km of relief in the western Andes  
551 (30 S) revealed by clumped isotope thermometry. *Earth and Planetary Science Letters*, 441, 188-199.
- 552 Burgener, L. K., Huntington, K. W., Sletten, R., Watkins, J. M., Quade, J., & Hallet, B. (2018). Clumped  
553 isotope constraints on equilibrium carbonate formation and kinetic isotope effects in freezing soils.  
554 *Geochimica et Cosmochimica Acta*, 235, 402-430.

- 555 Caves, J. K., Winnick, M. J., Graham, S. A., Sjostrom, D. J., Mulch, A., & Chamberlain, C. P. (2015). Role  
556 of the westerlies in Central Asia climate over the Cenozoic. *Earth and Planetary Science Letters*, 428, 33-43.
- 557 Cerling, T. E., Solomon, D. K., Quade, J. A. Y., & Bowman, J. R. (1991). On the isotopic composition of  
558 carbon in soil carbon dioxide. *Geochimica et Cosmochimica Acta*, 55(11), 3403-3405.
- 559 Clift, P. D., Hodges, K. V., Heslop, D., Hannigan, R., Van Long, H., & Calves, G. (2008). Correlation of  
560 Himalayan exhumation rates and Asian monsoon intensity. *Nature geoscience*, 1(12), 875-880.
- 561 Colin, C., Bertaux, J., Turpin, L., & Kissel, C. (2001). Dynamique de l'érosion dans le bassin versant de  
562 l'Irrawaddy au cours des deux derniers cycles climatiques (280–0 ka). *Comptes Rendus de l'Académie des  
563 Sciences-Series IIA-Earth and Planetary Science*, 332(8), 483-489.
- 564 DiNezio, P. N., Tierney, J. E., Otto-Bliesner, B. L., Timmermann, A., Bhattacharya, T., Rosenbloom, N., &  
565 Brady, E. (2018). Glacial changes in tropical climate amplified by the Indian Ocean. *Science advances*,  
566 4(12), eaat9658.
- 567 Ehleringer, J. R., Lin, Z. F., Field, C. B., Sun, G. C., & Kuo, C. Y. (1987). Leaf carbon isotope ratios of  
568 plants from a subtropical monsoon forest. *Oecologia*, 72(1), 109-114.
- 569 Fang, X., Dupont-Nivet, G., Wang, C., Song, C., Meng, Q., Zhang, W., ... & Chen, Y. (2020). Revised  
570 chronology of central Tibet uplift (Lunpola Basin). *Science Advances*, 6(50), eaba7298.
- 571 Fick, S. E., & Hijmans, R. J. (2017). WorldClim 2: new 1-km spatial resolution climate surfaces for global  
572 land areas. *International journal of climatology*, 37(12), 4302-4315.
- 573 Fischer-Femal, B. J., & Bowen, G. J. (2021). Coupled carbon and oxygen isotope model for pedogenic  
574 carbonates. *Geochimica et Cosmochimica Acta*, 294, 126-144.
- 575 Gallagher, T. M., & Sheldon, N. D. (2016). Combining soil water balance and clumped isotopes to  
576 understand the nature and timing of pedogenic carbonate formation. *Chemical Geology*, 435, 79-91.
- 577 Gallagher, T. M., Hren, M., & Sheldon, N. D. (2019). The effect of soil temperature seasonality on climate  
578 reconstructions from paleosols. *American Journal of Science*, 319(7), 549-581.
- 579 Gentis, N., Boura, A., & De Franceschi, D. (2019). Fossil wood from the Miocene of Myanmar: application  
580 to the reconstruction of monsoonal paleoenvironments. *Congrès Agora paleobotanica*, Jul 2019, Lille,  
581 France. [note: a scientific paper based on this conference talk is in review at *Geodiversitas* and available on  
582 ESSOAR: <https://www.essoar.org/doi/abs/10.1002/essoar.10506983.1>].
- 583 Hanpattanakit, P., Leclerc, M. Y., Mcmillan, A. M., Limtong, P., Maeght, J. L., Panuthai, S., ... &  
584 Chidthaisong, A. (2015). Multiple timescale variations and controls of soil respiration in a tropical dry  
585 dipterocarp forest, western Thailand. *Plant and soil*, 390(1), 167-181.

- 586 Hoke, G. D., Liu-Zeng, J., Hren, M. T., Wissink, G. K., & Garziona, C. N. (2014). Stable isotopes reveal  
587 high southeast Tibetan Plateau margin since the Paleogene. *Earth and Planetary Science Letters*, *394*, 270-  
588 278.
- 589 Huth, T. E., Cerling, T. E., Marchetti, D. W., Bowling, D. R., Ellwein, A. L., & Passey, B. H. (2019).  
590 Seasonal bias in soil carbonate formation and its implications for interpreting high-resolution paleoarchives:  
591 Evidence from southern Utah. *Journal of Geophysical Research: Biogeosciences*, *124*(3), 616-632.
- 592 Ingalls, M., Rowley, D., Olack, G., Currie, B., Li, S., Schmidt, J., ... & Colman, A. (2018). Paleocene to  
593 Pliocene low-latitude, high-elevation basins of southern Tibet: Implications for tectonic models of India-Asia  
594 collision, Cenozoic climate, and geochemical weathering. *GSA Bulletin*, *130*(1-2), 307-330.
- 595 Kelson, J. R., Huntington, K. W., Schauer, A. J., Saenger, C., & Lechler, A. R. (2017). Toward a universal  
596 carbonate clumped isotope calibration: Diverse synthesis and preparatory methods suggest a single  
597 temperature relationship. *Geochimica et Cosmochimica Acta*, *197*, 104-131.
- 598 Kelson, J. R., Huntington, K. W., Breecker, D. O., Burgener, L. K., Gallagher, T. M., Hoke, G. D., &  
599 Petersen, S. V. (2020). A proxy for all seasons? A synthesis of clumped isotope data from Holocene soil  
600 carbonates. *Quaternary Science Reviews*, *234*, 106259.
- 601 Khaing, T. T., Pasion, B. O., Lapuz, R. S., & Tomlinson, K. W. (2019). Determinants of composition,  
602 diversity and structure in a seasonally dry forest in Myanmar. *Global Ecology and Conservation*, *19*, e00669.
- 603 Kim, S. T., & O'Neil, J. R. (1997). Equilibrium and nonequilibrium oxygen isotope effects in synthetic  
604 carbonates. *Geochimica et cosmochimica acta*, *61*(16), 3461-3475.
- 605 Kohn, M. J. (2010). Carbon isotope compositions of terrestrial C3 plants as indicators of (paleo) ecology and  
606 (paleo) climate. *Proceedings of the National Academy of Sciences*, *107*(46), 19691-19695.
- 607 Kume, T., Tanaka, N., Yoshifuji, N., Chatchai, T., Igarashi, Y., Suzuki, M., & Hashimoto, S. (2013). Soil  
608 respiration in response to year-to-year variations in rainfall in a tropical seasonal forest in northern Thailand.  
609 *Ecohydrology*, *6*(1), 134-141.
- 610 Lai Lai Aung, Ei Ei Zin, Pwint Theingi, Naw Elvera, Phyu Phyu Aung, Thu Thu Han, Yamon Oo, &  
611 Skaland R.G. (2017). Myanmar Climate Report, *MET Report No. 9/2017*.
- 612 Licht, A., Cojan, I., Caner, L., Soe, A. N., Jaeger, J. J., & France-Lanord, C. (2014). Role of permeability  
613 barriers in alluvial hydromorphic palaeosols: the Eocene Pondaung Formation, Myanmar. *Sedimentology*,  
614 *61*(2), 362-382.
- 615 Licht, A., Van Cappelle, M., Abels, H. A., Ladant, J. B., Trabucho-Alexandre, J., France-Lanord, C., ... &  
616 Terry Jr, D. (2014b). Asian monsoons in a late Eocene greenhouse world. *Nature* *513*, 501-506.

- 617 Licht, A., Dupont-Nivet, G., Meijer, N., Rugenstein, J. C., Schauer, A., Fiebig, J., ... & Guo, Z. (2020).  
618 Decline of soil respiration in northeastern Tibet through the transition into the Oligocene icehouse.  
619 *Palaeogeography, Palaeoclimatology, Palaeoecology*, 560, 110016.
- 620 Liu, G., Li, X., Chiang, H. W., Cheng, H., Yuan, S., Chawchai, S., ... & Wang, X. (2020). On the glacial-  
621 interglacial variability of the Asian monsoon in speleothem  $\delta^{18}\text{O}$  records. *Science advances*, 6(7), eaay8189.
- 622 Meena, A., Hanief, M., Dinakaran, J., & Rao, K. S. (2020). Soil moisture controls the spatio-temporal pattern  
623 of soil respiration under different land use systems in a semi-arid ecosystem of Delhi, India. *Ecological*  
624 *Processes*, 9(1), 1-13.
- 625 Montanez, I. P. (2013). Modern soil system constraints on reconstructing deep-time atmospheric CO<sub>2</sub>.  
626 *Geochimica et Cosmochimica Acta*, 101, 57-75.
- 627 Page, M., Licht, A., Dupont-Nivet, G., Meijer, N., Barbolini, N., Hoorn, C., ... & Guo, Z. (2019).  
628 Synchronous cooling and decline in monsoonal rainfall in northeastern Tibet during the fall into the  
629 Oligocene icehouse. *Geology*, 47(3), 203-206.
- 630 Peters, N. A., Huntington, K. W., & Hoke, G. D. (2013). Hot or not? Impact of seasonally variable soil  
631 carbonate formation on paleotemperature and O-isotope records from clumped isotope thermometry. *Earth*  
632 *and Planetary Science Letters*, 361, 208-218.
- 633 Pivnik, D. A., Nahm, J., Tucker, R. S., Smith, G. O., Nyein, K., Nyunt, M., & Maung, P. H. (1998).  
634 Polyphase deformation in a fore-arc/back-arc basin, Salin subbasin, Myanmar (Burma). *AAPG bulletin*,  
635 82(10), 1837-1856.
- 636 Quade, J., Breecker, D. O., Daëron, M., & Eiler, J. (2011). The paleoaltimetry of Tibet: An isotopic  
637 perspective. *American Journal of Science*, 311(2), 77-115.
- 638 Quade, J., Eiler, J., Daëron, M., & Achyuthan, H. (2013). The clumped isotope geothermometer in soil and  
639 paleosol carbonate. *Geochimica et Cosmochimica Acta*, 105, 92-107.
- 640 Railsback, L. B. (2021). Pedogenic carbonate nodules from a forested region of humid climate in central  
641 Tennessee, USA, and their implications for interpretation of C3-C4 relationships and seasonality of meteoric  
642 precipitation from carbon isotope ( $\delta^{13}\text{C}$ ) data. *CATENA*, 200, 105169.
- 643 Reichle, R., G. De Lannoy, R. D. Koster, W. T. Crow, J. S. Kimball, and Q. Liu. 2018. SMAP L4 Global 3-  
644 hourly 9 km EASE-Grid Surface and Root Zone Soil Moisture Analysis Update, Version 4. Boulder,  
645 Colorado USA. *NASA National Snow and Ice Data Center Distributed Active Archive Center*.  
646 <https://doi.org/10.5067/60HB8VIP2T8W>. [Date Accessed].
- 647 Retallack, G. J. (2005). Pedogenic carbonate proxies for amount and seasonality of precipitation in paleosols.

- 648 *Geology*, 33(4), 333-336.
- 649 Romanek, C. S., Grossman, E. L., & Morse, J. W. (1992). Carbon isotopic fractionation in synthetic  
650 aragonite and calcite: effects of temperature and precipitation rate. *Geochimica et cosmochimica acta*, 56(1),  
651 419-430.
- 652 Rubio, V. E., & Detto, M. (2017). Spatiotemporal variability of soil respiration in a seasonal tropical forest.  
653 *Ecology and evolution*, 7(17), 7104-7116.
- 654 Saraswat, R., Lea, D. W., Nigam, R., Mackensen, A., & Naik, D. K. (2013). Deglaciation in the tropical  
655 Indian Ocean driven by interplay between the regional monsoon and global teleconnections. *Earth and*  
656 *Planetary Science Letters*, 375, 166-175.
- 657 Singh, L., & Singh, S. (1972). Chemical and morphological composition of kankar nodules in soils of the  
658 Vindhyan region of Mirzapur, India. *Geoderma*, 7(3-4), 269-276.
- 659 Stamp, L. D. (1940). The Irrawaddy River. *The Geographical Journal*, 95(5), 329-352.
- 660 Steinhorsdottir, M., Coxall, H. K., de Boer, A. M., Huber, M., Barbolini, N., Bradshaw, C. D., ... &  
661 Strömberg, C. A. E. (2020). The Miocene: the Future of the Past. *Paleoceanography and Paleoclimatology*,  
662 e2020PA004037.
- 663 Toumoulin, A., Tardif, D., Donnadiou, Y., Licht, A., Ladant, J. B., Kunzmann, L., & Dupont-Nivet, G.  
664 (2021). Evolution of continental temperature seasonality from the Eocene greenhouse to the Oligocene  
665 icehouse-A model-data comparison. *Climate of the Past Discussions*, 1-30. ([https://doi.org/10.5194/cp-2021-](https://doi.org/10.5194/cp-2021-27)  
666 27)
- 667 Van Der Kaars, S., & Dam, R. (1997). Vegetation and climate change in West-Java, Indonesia during the last  
668 135,000 years. *Quaternary International*, 37, 67-71.
- 669 Westerweel, J., Licht, A., Cogné, N., Roperch, P., Dupont-Nivet, G., Kay Thi, M., ... & Wa Aung, D. (2020).  
670 Burma Terrane collision and northward indentation in the Eastern Himalayas recorded in the Eocene-  
671 Miocene Chindwin Basin (Myanmar). *Tectonics*, 39(10), e2020TC006413.
- 672 Xiong, Z., Ding, L., Spicer, R. A., Farnsworth, A., Wang, X., Valdes, P. J., ... & Yue, Y. (2020). The early  
673 Eocene rise of the Gonjo Basin, SE Tibet: From low desert to high forest. *Earth and Planetary Science*  
674 *Letters*, 543, 116312.

Localities			Climate parameters from WorldClim V2, res: 5min				Clumped isotopic data									
age	location on fig. 1	name	MAT (in °C)	WMMT (in °C)	CMMT (in °C)	MAP (in mm)	<i>n</i>	Carbonate $\delta^{13}\text{C}$ (‰ VPDB)	$\delta^{13}\text{C}$ S.E. (‰ VPDB)	Carbonate $\delta^{18}\text{O}$ (‰ VPDB)	$\delta^{18}\text{O}$ S.E. (‰ VPDB)	$\Delta_{47}$ Intercarb acid (‰)	$\Delta_{47}$ S.E. (‰)	$T\Delta_{47}$ (°C)	$T\Delta_{47}$ S.E. (°C)	Soil Water $\delta^{18}\text{O}$ (‰ VSMOW)
Quaternary soils	1	17NOD01	27.2	31.3	21.2	747	8	-6.08	0.02	-4.56	0.16	0.6904	0.0092	22.1	3.0	-2.8
	2	17NOD04	25.1	29.6	19.9	772	11	-6.97	0.04	-10.11	0.02	0.6943	0.0099	20.9	3.2	-8.6
	3	19NOD02	24.3	28.5	18.1	1701	6	-10.18	0.02	-4.39	0.03	0.6898	0.0107	22.3	3.5	-2.6
	3	19NOD03	24.3	28.5	18.1	1701	7	-10.16	0.03	-6.71	0.07	0.6965	0.0099	20.2	3.1	-5.3
	4	19NOD04	25.7	29.8	19.5	1372	9	-14.72	0.01	-4.07	0.03	0.7056	0.0097	17.3	3.0	-3.3
							4	-13.92	0.01	-4.00	0.02	0.6806	0.0073	25.4	2.4	-1.5
	5	19NOD06	25.7	30.0	20.0	845	7	-8.44	0.02	-7.44	0.03	0.7140	0.0099	14.7	3.0	-7.2
							6	-8.33	0.01	-6.63	0.07	0.6862	0.0059	23.5	2.0	-4.6
	6	19NOD07	27.6	31.9	22.1	647	10	-6.97	0.01	-6.85	0.03	0.7072	0.0092	16.8	2.8	-6.2
	5	19NOD08	27	31.3	21.3	720	10	-6.48	0.02	-8.86	0.13	0.7061	0.0121	17.1	3.7	-8.1
	7	19NOD09	27.3	31.6	21.9	655	7	-7.57	0.06	-7.36	0.07	0.7111	0.0099	15.6	3.0	-7.0
	8	20NOD01	27	31.5	20.9	869	7	-7.70	0.09	-5.43	0.07	0.0096	0.0099	22.2	3.2	-3.6
	9	20NOD03	26.8	31.0	21.4	723	8	-9.89	0.02	-8.59	0.06	0.7063	0.0093	17.1	2.9	-7.9
4							-9.19	0.01	-7.07	0.03	0.6965	0.0073	20.2	2.3	-5.7	
Early Miocene	3	19NAT13	N/A				8	-9.70	0.48	-4.13	0.90	0.6976	0.0121	19.8	3.8	-2.8
	3	19NAT01	N/A				5	-9.91	0.06	-1.63	0.05	0.6881	0.0091	22.9	3.0	0.3

Figure 6.

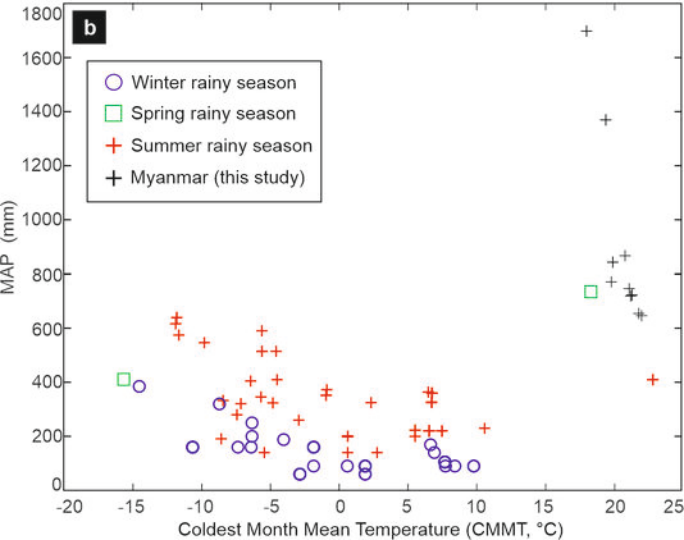
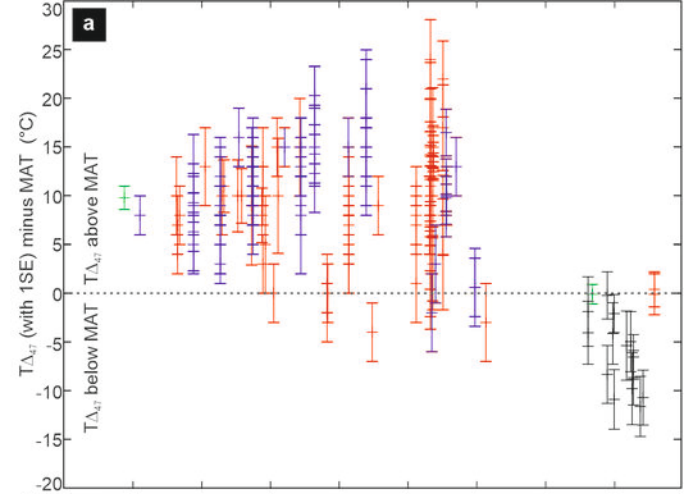


Figure 2.

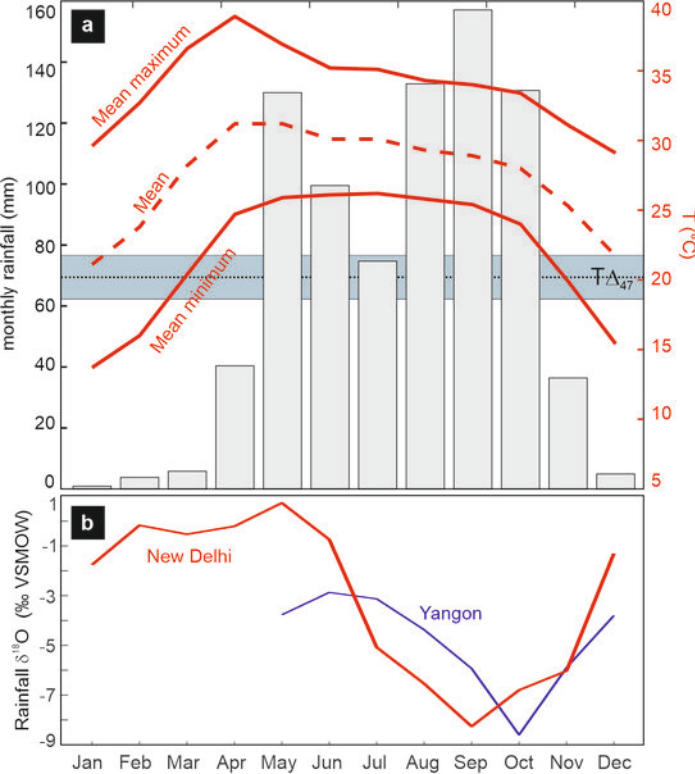


Figure 1.

- + Climate station
- 200 mm isohyets
- Late Quaternary soil samples
- Early Miocene paleosols



CB

3

4

5

6

7

8

9

1

2

150 km

Summer monsoonal moisture

Figure 5.

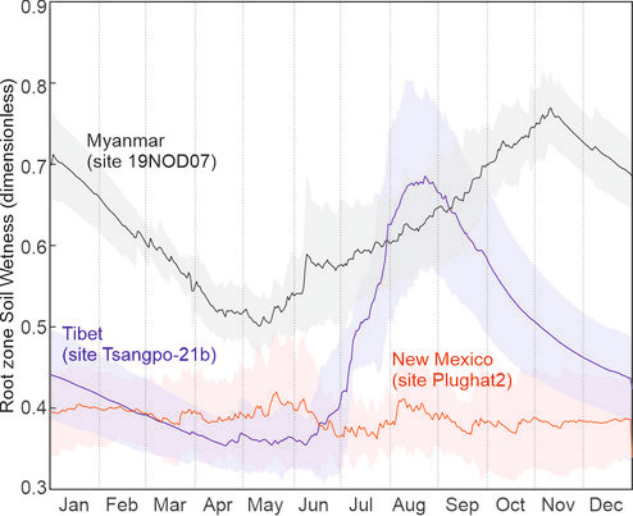


**Figure 4.**

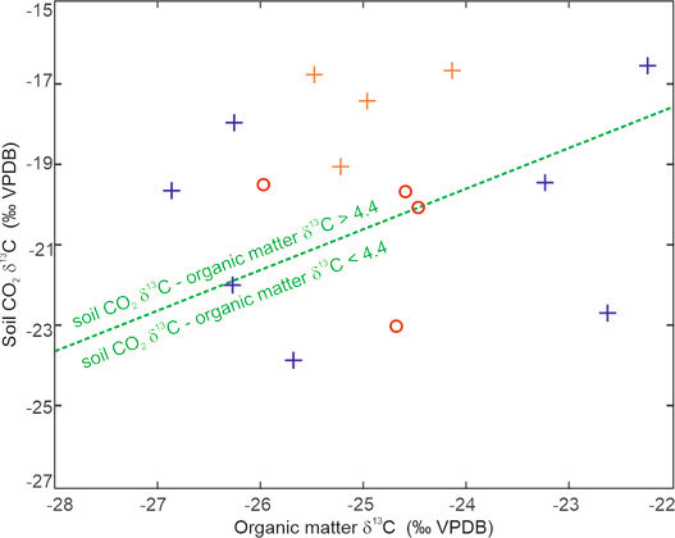


Figure 3.

